

Current-density inhomogeneity throughout the thickness of superconducting films and its effect on their irreversible magnetic properties

R. Prozorov

Institute of Superconductivity, Department of Physics, Bar-Ilan University, 52900 Ramat-Gan, Israel

E. B. Sonin

*The Racah Institute of Physics, The Hebrew University of Jerusalem, Jerusalem 91904, Israel
and Ioffe Physical Technical Institute, St. Petersburg 194021, Russia*

E. Sheriff, A. Shaulov, and Y. Yeshurun

*Institute of Superconductivity, Department of Physics, Bar-Ilan University, 52900 Ramat-Gan, Israel
(Received 29 April 1997; revised manuscript received 17 February 1998)*

We calculate the distribution of the current density j in superconducting films along the direction of an external field applied perpendicular to the film plane. Our analysis reveals that in the presence of bulk pinning j is inhomogeneous on a length scale of the order of the intervortex distance. This inhomogeneity is significantly enhanced in the presence of surface pinning. We introduce a critical state model, which takes into account the current-density variations throughout the film thickness, and show how these variations give rise to the experimentally observed thickness dependence of j and magnetic relaxation rate.

[S0163-1829(98)03121-X]

I. INTRODUCTION

The magnetic behavior of type-II superconductors depends strongly on the sample shape.¹⁻⁸ Significant progress has recently been made in understanding the effects of a sample aspect ratio on its magnetic behavior,¹ in particular, in the case of thin films with the magnetic field normal to the film plane (“perpendicular geometry”).^{2,3} Theory¹⁻⁴ and experiment^{5,6} show that the magnetic behavior in the perpendicular geometry has many distinctive features, essentially different from the parallel geometry, e.g., a more complicated structure of the critical state and the presence of geometrical barriers.⁷

A number of elegant analytical solutions for the perpendicular geometry (for strips and disks) describe the Meissner,⁸ the mixed state,^{1,3} and magnetic flux creep.² These solutions are based on the important ansatz that one can treat the film as an infinitesimal thin plane. Then, current distribution related to vortex bending does not influence the results of the analysis that deals only with the current density and the vortex displacements averaged over the film thickness. This approach was very successful in explaining the peculiarities of the current density and the magnetic induction distribution across the film plane. However, this approach cannot account for any *thickness dependence* of both persistent current density j (Refs. 6 and 9–12) and magnetic relaxation rate^{11,12} in thin films.

Explanation of the observed decrease of j with the increase of the film thickness d is usually based on the idea that pinning on surfaces *perpendicular* to the direction of vortices is strong enough and must be taken into account.^{4,6,9} However, as we demonstrate below, this is not sufficient for understanding the thickness dependence of the magnetic relaxation rate, which was found to decrease with the increase of the film thickness.^{11,12}

Another explanation of the observed thickness dependence of the current density may be based on collective pinning in a two-dimensional (2D) regime, i.e., for longitudinal correlation length L larger than the film thickness. This case is carefully considered in Ref. 13. In a 2D collective pinning regime, the pinning is stronger for thinner samples. As a result, in this model both the critical-current density and the creep barrier are larger in thinner samples, contrary to the experimental results. Also, this scenario is probably not relevant for the explanation of the experimental data discussed below, because the thickness of our films $d \geq 800 \text{ \AA}$ is larger than $L \approx 40 - 100 \text{ \AA}$.

In order to understand the experimental results, we calculate the current density and magnetic induction distribution by using the “two-mode electrodynamics” theory suggested earlier to explain the ac response in bulk materials.¹⁵ The essence of this theory is that two length scales govern the penetration of fields and currents into type-II superconductors. The longer scale is of electrodynamic origin and, therefore, is more universal: it exists, for example, in a superconductor in the Meissner state (the London penetration depth) or, in a normal conductor (the skin depth). The shorter scale is related to the vortex-line tension, so it is unique for a type-II superconductor in the mixed state. This scale was introduced into the continuous theory of type-II superconductors by Matheiu and Simon¹⁶ (see also Refs. 17 and 18). When applying the two-mode electrodynamics to the critical state one may ignore the time variation, i.e., the two-mode electrodynamics becomes the *two-mode electrostatics* theory.

Our analysis of a type-II thin superconducting film within the two-mode electrostatics theory leads to the conclusion that for strong enough bulk pinning, inhomogeneity of the current density becomes important, even in the absence of surface pinning, if the film thickness exceeds the Campbell

penetration depth λ_c . Thus, inhomogeneity of the current distribution throughout the film thickness is a *distinctive* and inevitable feature of the perpendicular film geometry like, for example, the geometrical barrier.⁷ Inhomogeneity of the current distribution is significantly enhanced if the critical state is supported by the surface pinning. In this case, most of the current is confined to a layer of a depth of the order of the intervortex distance, which is usually much smaller than the London penetration depth λ and film thickness. As a result of this inhomogeneity, the *measured* average critical current density becomes thickness dependent. This current inhomogeneity also causes a thickness dependence of the magnetic relaxation rate. In the following we present detailed calculations of the distribution of the current density j and induction field B in thin type-II superconducting film, resulting from surface and/or bulk pinning. We then introduce the first critical state model that takes into account the variation in j throughout the film thickness. Calculations based on this critical state model lead to a thickness dependence in j and magnetic relaxation rate. These predictions are compared with the experimental data.

II. THEORY

A. Equations of electrodynamics for the mixed state in perpendicular geometry

Let us consider a thin superconducting strip, infinitely long in the y direction, with width $2w$ ($-w < x < w$) and thickness $2d$ ($-d < z < d$). External magnetic field H is applied along the z axis, perpendicular to the film plane. The vortex density n is determined by the z component B_z of the average magnetic field (magnetic induction) \vec{B} in the film: $n = B_z / \Phi_0$. Supercurrent of density $I_y(x, z)$ flows along the y axis resulting in a Lorenz force in the x direction, and a vortex displacement u along the x axis.

We begin with the electrodynamic equations describing the mixed state of type-II superconductors in such a geometry. They include the London equation for the x component of the magnetic field

$$B_x - \lambda^2 \frac{\partial^2 B_x}{\partial z^2} = B_z \frac{\partial u}{\partial z}, \quad (1)$$

the Maxwell equation

$$\frac{4\pi}{c} j_y = \frac{\partial B_x}{\partial z} - \frac{\partial B_z}{\partial x}, \quad (2)$$

and the equation of vortex motion

$$\eta \frac{\partial u}{\partial t} + ku = \frac{\Phi_0}{c} j_y + \frac{\Phi_0}{4\pi} H^* \frac{\partial^2 u}{\partial z^2}, \quad (3)$$

where

$$H^* = \frac{\Phi_0}{4\pi\lambda^2} \ln \frac{a_0}{r_c} \quad (4)$$

is a field of order of the first critical field H_{c1} , $a_0 \approx \sqrt{\Phi_0/B_z}$ is the intervortex distance, and $r_c \sim \xi$ is an effective vortex core radius. The equation of the vortex motion

arises from the balance among four terms: (i) the friction force proportional to the friction coefficient η ; (ii) the homogeneous, linear elastic pinning force $\propto k$ (i.e., assuming small displacements u); (iii) the Lorentz force proportional to the current density j ; and (iv) the vortex-line tension force [the last term on the right-hand side of Eq. (3)], taken from Ref. 15.

In the parallel geometry, ($d \rightarrow \infty$), vortices move without bending so that the x component B_x is absent, and the Maxwell equation becomes $4\pi j_y/c = -\partial B_z/\partial x$. Since B_z is proportional to the vortex density, this current may be called a *diffusion current*. The case of the perpendicular geometry ($d \ll w$) is essentially different: the diffusion current is small compared to the *bending current* $\partial B_x/\partial z$ (see the estimation below) and may be neglected for calculation of the distribution throughout the film thickness (along the z axis). As a result, Eq. (3) becomes

$$\eta \frac{\partial u}{\partial t} + ku = \frac{\Phi_0}{4\pi} \frac{\partial B_x}{\partial z} + \frac{\Phi_0}{4\pi} H^* \frac{\partial^2 u}{\partial z^2}. \quad (5)$$

Equations (1) and (5) determine the distribution of the displacement $u(z)$ and of the in-plane magnetic induction $B_x(z)$. This also yields a distribution of the current density ($4\pi/c$) $j_y(z) = \partial B_x(z)/\partial z$. But these equations are still not closed, since the two components of the magnetic induction, B_x and B_z , and current density $j_y(z)$ are connected by the Biot-Savart law. However, neglecting the diffusion current in the Maxwell equation we separate the problem into two parts: (1) determination of the distribution of fields and currents along the z axis, taking the total current $I_y = cB_x^s/2\pi$ [here $B_x^s \equiv B_x(z=d)$] and the perpendicular magnetic-induction component B_z as free parameters; (2) determination of the parameters I_y and B_z using the Biot-Savart law. The latter part of the problem (solution of the integral equation given by the Biot-Savart law) has already been studied carefully in previous works.^{1,3} In the present work we concentrate on the analysis of the distribution of fields and currents throughout the film thickness (z dependence).

The accuracy of our approach is determined by the ratio of the diffusion current $\partial B_z/\partial x$ to the bending current $\partial B_x/\partial z$, since we neglect the diffusion current contribution to the total current. Suppose, as a rough estimation, that $B_z \sim B_x$.⁵ Then, the diffusion current density is roughly $\sim I_y/w$, whereas the bending current density is $\sim I_y/d$.^{1,3,5,7} Thus, the ratio between the diffusion and the bending current is approximately $d/w \sim 10^{-3} \div 10^{-4}$ for typical thin films. Note that this condition does not depend on the magnitude of the critical current and is well satisfied also in typical single crystals, where $d/w \sim 0.01 \div 0.1$. Therefore, the results we obtain below hold for a wide range of typical samples used in the experiment.

B. Two-mode electrostatics: Two length scales

Let us consider the static case when vortices do not move, hence there is no friction. Then, Eq. (5) becomes

$$ku = \frac{\Phi_0}{4\pi} \frac{\partial B_x}{\partial z} + \frac{\Phi_0}{4\pi} H^* \frac{\partial^2 u}{\partial z^2}. \quad (6)$$

Excluding the B_x component of the magnetic induction from Eqs. (1) and (6) we obtain the equation for the vortex displacement:

$$-\frac{4\pi k}{\Phi_0} \left(u - \lambda^2 \frac{\partial^2 u}{\partial z^2} \right) + (H^* + B_z) \frac{\partial^2 u}{\partial z^2} - \lambda^2 H^* \frac{\partial^4 u}{\partial z^4} = 0. \quad (7)$$

The two length scales that govern distributions over the z axis become evident if one tries to find a general solution of Eq. (7) in the form $B_x \sim u \sim \exp(ipz)$. Then, the dispersion equation for p is biquadratic and yields two negative values for p^2 . In the limit $k \ll 4\pi\lambda^2/\Phi_0(H^* + B_z)$ (weak bulk pinning):

$$p_1^2 = -\frac{1}{\tilde{\lambda}^2} = -\frac{1}{\lambda^2} \frac{H^* + B_z}{H^*}, \quad (8)$$

$$p_2^2 = -\frac{1}{\lambda_C^2} = -\frac{4\pi k}{\Phi_0(H^* + B_z)}. \quad (9)$$

Thus, the distribution along the z axis is characterized by the two length scales: the Campbell length λ_C , which is the electrodynamic length, and length $\tilde{\lambda}$, given by Eq. (8), which is related to λ and the vortex-line tension.

C. Current density and field distribution

In order to determine distribution of currents and fields throughout the film thickness, one must add the proper boundary conditions to the general solution of Eq. (7). We look for a solution which is a superposition of two modes. In particular, for the vortex displacement we can write

$$u(z) = u_0 \cosh \frac{z}{\lambda_C} + u_1 \cosh \frac{z}{\tilde{\lambda}}. \quad (10)$$

Using Eq. (6) one has for the current density:

$$\frac{4\pi}{c} j_y = \frac{\partial B_x}{\partial z} \approx B_z \frac{u_0}{\lambda_C^2} \cosh \frac{z}{\lambda_C} - H^* \frac{u_1}{\tilde{\lambda}^2} \cosh \frac{z}{\tilde{\lambda}}. \quad (11)$$

The total current is

$$\frac{4\pi}{c} I_y = 2B_x(d) = 2B_z \frac{u_0}{\lambda_C} \sinh \frac{d}{\lambda_C} - 2H^* \frac{u_1}{\tilde{\lambda}} \sinh \frac{d}{\tilde{\lambda}}. \quad (12)$$

Equation (12) is in fact a boundary condition imposed on the amplitudes of two modes, u_0 and u_1 . The second boundary condition is determined by the strength of the surface pinning. If displacements are small, the general form of this boundary condition is

$$\alpha u(\pm d) \pm \frac{\partial u}{\partial z} \Big|_{\pm d} = 0, \quad (13)$$

where $\alpha=0$ in the absence of surface pinning and $\alpha \rightarrow \infty$ in the limit of strong surface pinning. In the following parts of the section we consider these two limits.

1. Surface pinning

Let us consider the case of surface pinning in the absence of bulk pinning ($k=0$), when the Campbell length $\lambda_C \rightarrow \infty$ [see Eq. (9)]. By ‘‘surface pinning’’ we understand pinning due to surface roughness on the surfaces *perpendicular* to the vortex direction. The surface roughness is assumed to be much smaller than the film thickness d . By substituting $\lambda_C \rightarrow \infty$ in the general solution Eq. (10), we derive the displacement for surface pinning:

$$u(z) = u_0 + u_1 \cosh \frac{z}{\tilde{\lambda}}, \quad (14)$$

where u_0 and u_1 are constants, which can be determined from the boundary conditions Eqs. (12) and (13). Note, however, that u_0 is not important in the case of surface pinning, because the constant u_0 does not affect distributions of currents and fields.

The magnetic field B_x is obtained from Eq. (6):

$$B_x(z) = -H^* \frac{u_1}{\tilde{\lambda}} \sinh \frac{z}{\tilde{\lambda}}, \quad (15)$$

and the current is determined from the Maxwell equation (2) neglecting the diffusion current:

$$j_y = -\frac{c}{4\pi} H^* \frac{u_1}{\tilde{\lambda}^2} \cosh \frac{z}{\tilde{\lambda}}. \quad (16)$$

It is important to note that the characteristic length $\tilde{\lambda}$, which varies between the London penetration length λ and the intervortex distance $a_0 \sim \sqrt{\Phi_0/B_z}$, is much smaller than λ for a dense vortex array, $B_z \gg H^*$. Taking into account that usually thin films have thickness less or equal to 2λ , the effect of the vortex bending due to surface pinning may be very important: most of the current is confined to a thin surface layer of width $\tilde{\lambda}$.

The current density on the surface is $j_s \equiv j_y(z=d) = -(c/4\pi)H^*(u_1/\tilde{\lambda}^2)\cosh(d/\tilde{\lambda})$. Thus,

$$u_1 = -\frac{4\pi}{c} \frac{\tilde{\lambda}^2 j_s}{H^* \cosh \frac{d}{\tilde{\lambda}}}. \quad (17)$$

The total current integrated over the film thickness $2d$ is

$$I_y = \int_{-d}^d j_y(z) dz = -\frac{c}{2\pi} H^* \frac{u_1}{\tilde{\lambda}} \sinh \frac{d}{\tilde{\lambda}} = 2\tilde{\lambda} j_s \tanh \frac{d}{\tilde{\lambda}}. \quad (18)$$

Thus, the *average* current density $j_a \equiv I_y/2d$ —the quantity derived in the experiment—decreases with thickness as

$$j_a = j_s \frac{\tilde{\lambda}}{d} \tanh \frac{d}{\tilde{\lambda}}, \quad (19)$$

yielding $j_a = j_s \tilde{\lambda}/d$ for $\tilde{\lambda}/d \ll 1$ as found experimentally.¹¹

The field and the current distribution over the film thickness are

$$j_y(z) = \frac{I_y}{2\tilde{\lambda}} \frac{\cosh \frac{z}{\tilde{\lambda}}}{\sinh \frac{z}{\tilde{\lambda}}} = j_s \frac{\cosh \frac{z}{\tilde{\lambda}}}{\cosh \frac{z}{\tilde{\lambda}}}, \quad (20)$$

$$B_x(z) = \frac{2\pi}{c} I_y \frac{\sinh \frac{z}{\tilde{\lambda}}}{\sinh \frac{z}{\tilde{\lambda}}} = \frac{4\pi}{c} j_s \tilde{\lambda} \frac{\sinh \frac{z}{\tilde{\lambda}}}{\cosh \frac{z}{\tilde{\lambda}}}. \quad (21)$$

Thus, the current penetrates into a small depth $\tilde{\lambda}$ and is exponentially small in the bulk beyond this length.

2. Bulk pinning

A remarkable feature of the perpendicular geometry is that, even in the absence of surface pinning, vortices are bent. This is in striking contrast with the parallel geometry where the diffusion current distribution is homogeneous along the direction of vortices and, therefore, does not bend them. Absence of surface pinning means that at the surface $\partial u / \partial z = 0$ (a vortex is perpendicular to an ideal surface). This yields the relation between u_0 and u_1 [see Eq. (10)]:

$$u_1 = -u_0 \frac{\tilde{\lambda}}{\lambda_C} \frac{\sinh \frac{z}{\lambda_C}}{\sinh \frac{z}{\tilde{\lambda}}}.$$

Then, Eq. (12) becomes

$$\frac{4\pi}{c} I_y = 2(B_z + H^*) \frac{u_0}{\lambda_C} \frac{d}{\lambda_C}. \quad (22)$$

The current distribution is

$$j_y(z) = I_y \left(\frac{1}{2\lambda_C} \frac{B_z}{H^* + B_z} \frac{\cosh \frac{z}{\lambda_C}}{\sinh \frac{z}{\lambda_C}} + \frac{1}{2\tilde{\lambda}} \frac{H^*}{H^* + B_z} \frac{\cosh \frac{z}{\tilde{\lambda}}}{\sinh \frac{z}{\tilde{\lambda}}} \right). \quad (23)$$

In the limit $d \ll \lambda_C$ Eq. (23) yields

$$j_y(z) = I_y \left(\frac{1}{2d} \frac{B_z}{H^* + B_z} + \frac{1}{2\tilde{\lambda}} \frac{H^*}{H^* + B_z} \frac{\cosh \frac{z}{\tilde{\lambda}}}{\sinh \frac{z}{\tilde{\lambda}}} \right). \quad (24)$$

Another interesting case is that of the dense vortex array, $B_z \gg H^*$:

$$j_y(z) = \frac{I_y}{2\lambda_C} \frac{\cosh \frac{z}{\lambda_C}}{\sinh \frac{z}{\lambda_C}} = j_s \frac{\cosh \frac{z}{\lambda_C}}{\cosh \frac{z}{\lambda_C}}, \quad (25)$$

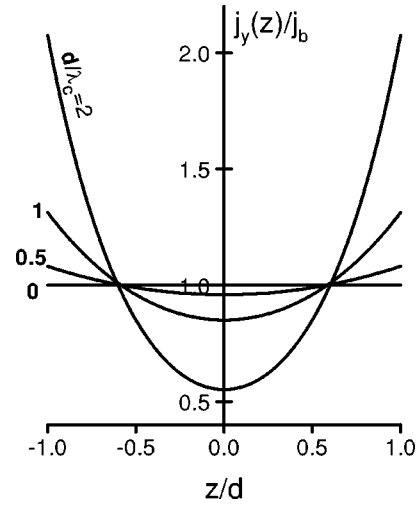


FIG. 1. Current-density distribution vs normalized depth z/d for the indicated d/λ_c ratios. The current distribution becomes more inhomogeneous as the ratio d/λ_c increases.

where again j_s is the current density on the film surface. Remarkably, current density is inhomogeneous even in the absence of surface pinning. We illustrate this in Fig. 1, where we plot $j_y(z)/j_b$ vs z/d at different ratios d/λ_c . ‘‘Uniform’’ bulk current density $j_b = I_y/2d$ corresponds to the limit $d/\lambda_c = 0$. Physically, such current profiles reflect Meissner screening of the in-plane component B_x of the self-field.

For the average current density we have

$$j_a = j_s \frac{\lambda_C}{d} \tanh \frac{d}{\lambda_C}, \quad (26)$$

which is similar to the case of the surface pinning, Eq. (19), with $\tilde{\lambda}$ replaced by λ_C .

Thus, in the perpendicular geometry, the current distribution is strongly inhomogeneous: the whole current is confined to a narrow surface layer of width $\tilde{\lambda}$ (surface pinning), or λ_C (bulk pinning).

D. Critical state

In the theory given in the previous sections we have assumed that currents and vortex displacements are small. In this section we deal with the critical state when the current density equals its critical value j_c . Let us consider how it can affect our picture, derived in the previous sections for small currents.

1. Surface pinning

If vortices are pinned only at the surface, the value of the critical current depends on the profile of the surface, and one may not use the linear boundary condition imposed on the vortex displacement, Eq. (13). However, the z -independent vortex displacement u_0 does not influence the current density and field distribution in the bulk as shown in Sec. II C 1 [see Eqs. (15) and (16)]. Therefore the bulk current density and field distribution derived from our linear analysis can be used even for the critical state.

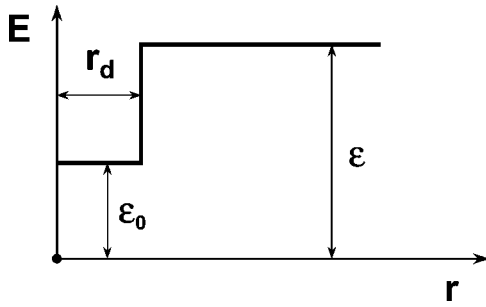


FIG. 2. Vortex energy (per unit length) in the vicinity of the pinning center of radius r_d .

2. Bulk pinning

In this case our theory must be modified for the critical state. In particular, for large currents the bulk pinning force becomes nonlinear and, as a result, the current and field penetration is not described by simple exponential modes. Formally, this nonlinearity may be incorporated into our theory assuming a u -dependent pinning constant k , thus allowing k to vary along the vortex line. As an example, let us consider the case of strongly localized pinning force when the vortex is pinned by a potential well of a small radius r_d like that sketched in Fig. 2: the vortex energy per unit length (vortex-line tension) is given by ε for vortex line segments outside the potential well and by ε_0 for segments inside the well. Thus, the pinning energy per unit length is $\varepsilon - \varepsilon_0$. In fact, such a potential well model may describe pinning of vortices by, for example, one-dimensional columnar defects or planar defects, such as twin or grain boundaries.^{19,20} The latter is relevant in thin films obtained by usual method of laser ablation. Therefore, we can also use such a pinning potential as a rough qualitative model for typical types of pinning sites, in order to illustrate the effect of bulk pinning on the current density distribution and the rate of magnetic relaxation in thin films.

If the current distribution were uniform, such a potential well would keep the vortex pinned until the current density j_y exceeds the critical value $c(\varepsilon - \varepsilon_0)/\Phi_0 r_d$. The escape of the trapped vortex line from the potential well occurs via formation of the untrapped circular segment of the vortex line [see Fig. 3(a)]. In this case, both the critical-current density and the energy barrier for vortex depinning do not depend on film thickness.¹⁹

But, in perpendicular geometry the current distribution is not homogeneous. In order to find it for the critical state, we may use the following approach. The vortex line consists of the trapped and untrapped segments as shown in Fig. 3(b). The untrapped segment is beyond the potential well, therefore there is no bulk pinning force acting on it. This means that the shape of this segment is described by Eq. (6) with $k=0$. Applying the theory of Sec. II C 1, one obtains that the total current $I_y = \int_{-d}^d j_y(z) dz$ is concentrated near the film surfaces within a narrow surface layer of width $\tilde{\lambda}$. Inside the surface layer the vortex line is curved, but has a straight segment of length L outside the layer, as illustrated in Fig. 3(b). As for the vortex-line segment trapped by the potential well, we assume that it is straight and vertical, neglecting its possible displacements inside the potential well. Formally speaking, our approach introduces a nonhomogeneous bulk-

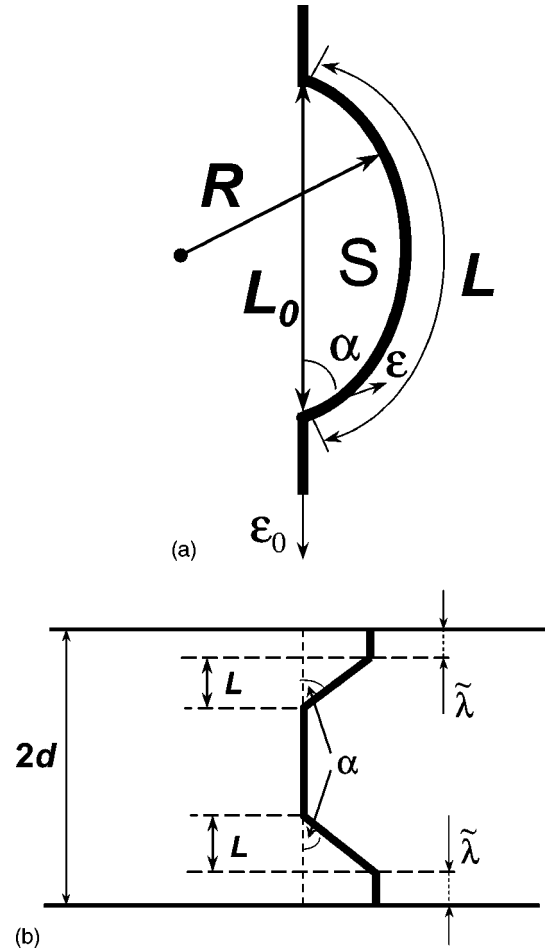


FIG. 3. (a) Vortex depinning by a uniform current. (b) Simple scenario of vortex depinning by nonhomogeneous current flowing in a layer $\tilde{\lambda}$.

pinning constant k assuming that $k=0$ for the untrapped segment and $k=\infty$ for the trapped one. The energy of the vortex line in this state is determined by the line tensions (ε and ε_0) and is given by

$$\begin{aligned} E &= 2\varepsilon \frac{L}{\cos\alpha} - 2\varepsilon_0 L - 2 \frac{\Phi_0}{c} I_y L \tan\alpha \\ &= 2L \tan\alpha \left(\varepsilon \sin\alpha - \frac{\Phi_0}{c} I_y \right), \end{aligned} \quad (27)$$

where the contact angle α is determined by the balance of the line-tension forces at the point where the vortex line meets the line defect:

$$\cos\alpha = \frac{\varepsilon_0}{\varepsilon}. \quad (28)$$

III. MAGNETIC RELAXATION

We now discuss the effect of current-density distribution on the thickness dependence of magnetic relaxation. We first show below, that uniform current density cannot explain the experimentally observed thickness dependence. We also show that the inhomogeneous current density distribution, resulting from the surface pinning only, also cannot explain

the experimental data. We demonstrate that only presence of a bulk pinning and the resulting current inhomogeneity may lead to an accelerated relaxation in thinner films. We finally discuss the general case when both bulk and surface pinning are present.

As pointed out above, if the current distribution is uniform throughout the film thickness, a trapped vortex may escape from the potential well (Fig. 2) via formation of a circular segment of the vortex line [Fig. 3(a)], with the energy

$$E = \varepsilon L - \varepsilon_0 L_0 - \frac{\Phi_0}{c} j_y S, \quad (29)$$

where L and L_0 are the lengths of the vortex line segment before and after formation of the loop, S is the area of the loop.^{20,19} If the loop is a circular arc of the radius R and the angle 2α [Fig. 3(a)], then $L_0 = 2R\sin\alpha$, $L = 2R\alpha$, and $S = \frac{1}{2}R^2(2\alpha - \sin 2\alpha)$, where the contact angle α is given by Eq. (28). Then,

$$\begin{aligned} E &= 2R(\varepsilon\alpha - \varepsilon_0\sin\alpha) - \frac{\Phi_0}{2c} j_y R^2(2\alpha - \sin 2\alpha) \\ &= (2\alpha - \sin 2\alpha) \left(\varepsilon R - \frac{\Phi_0}{2c} j_y R^2 \right). \end{aligned} \quad (30)$$

The height of the barrier is determined by the maximum energy at $R_c = \varepsilon c / \Phi_0 j_y$:

$$E_b = (2\alpha - \sin 2\alpha) \frac{\varepsilon^2 c}{2\Phi_0 j_y}. \quad (31)$$

As one might expect, this barrier and consequently the relaxation rate do not depend on the film thickness. We stress that this estimation is valid only for $d > R_c$. If $d < R_c$ the energy barrier is obtained from Eq. (30) by substituting $R = d$. This case of uniform current, however, leads to a thickness independent current density, and therefore cannot describe the experimental data.

A. Surface pinning

In this case, the whole current is confined to the surface layer of width $\tilde{\lambda}$. It is apparent from Eq. (9) that for typical experimental fields ($\sim 1T$) $\tilde{\lambda}$ is smaller than the film thickness. This means that current flows mostly in a thin surface layer. Thus, all creep parameters, including the creep barrier, are governed by the total current I_y , and not by the average current density $I_y/2d$. Then, apparently, the critical current density and the creep barrier are larger for thinner films, similar to the case of the collective-pinning effect mentioned above. Thus, also this scenario cannot explain the observed accelerated relaxations in the thinner films.

B. Short-range bulk pinning

Let us consider the relaxation process for a critical state supported by the short-range pinning force discussed in Sec. II D 2. The energy E of the vortex line is given by Eq. (27). The average critical current density corresponds to $E = 0$ and is inversely proportional to the film thickness [see also Eq. (26)]:

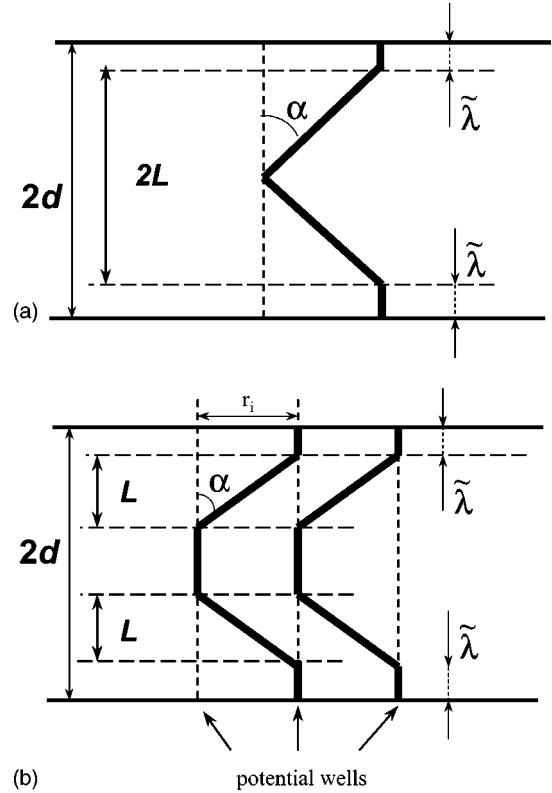


FIG. 4. (a) Barrier maximum configuration in the case of a dilute pinning centers. (b) Barrier maximum configuration in the case of the dense defects.

$$j_c = \frac{I_c}{2d} = \frac{c\varepsilon}{2d\Phi_0} \sin\alpha. \quad (32)$$

The energy barrier is given by the maximum energy at $d = L + \tilde{\lambda} \approx L$ when the whole vortex line has left the potential well [Fig. 4(a)]:

$$E_b = \tan\alpha \left(2d\varepsilon\sin\alpha - 4d^2 \frac{\Phi_0}{c} j_a \right), \quad (33)$$

where $j_a = I_y/2d$ is the average current density. If $j_c > j_a > j_c/2$, then $\partial E_b / \partial d < 0$, i.e., the barrier is larger for thinner films. But, for $j_a < j_c/2$ the derivative $\partial E_b / \partial d > 0$, and the barrier *increases* with the increase of the film thickness. Thus, under this condition ($j_a < j_c/2$) the magnetic relaxation rate is larger in the thinner samples.

The above analysis did not take into account the possibility for dense defects. By “dense” we mean that the distance r_i from the neighbor potential well is less than $d \tan\alpha$ [see Fig. 4(b)]. In this case the maximal energy (the barrier peak) is smaller than the barrier calculated in Eq. (33). Then the barrier energy is given by

$$E_b = r_i \left(2\varepsilon\sin\alpha - 4d \frac{\Phi_0}{c} j_a \right). \quad (34)$$

In this case $\partial E_b / \partial d < 0$ and the energy barrier for thinner films is always larger. Therefore one can see faster relaxation in thinner films only if the films are so thin that $d < r_i / \tan\alpha$ and the energy barrier is given by Eq. (33). From the experimental results shown below we infer that the aver-

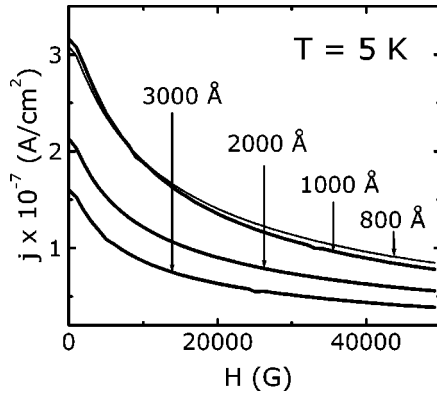


FIG. 5. Average persistent current density j_a as a function of magnetic field at $T=5$ K for films of different thickness.

age distance between effective defects $r_i \geq 1000$ Å in agreement with direct measurements using atomic force microscopy.

To conclude, if the average current density in thin films becomes small enough compared to the original critical current density and if the films are thin enough, the relaxation at the same average persistent current is predicted to be faster for the thinner films.

C. General case

In the simplified picture of the critical-state relaxation outlined in the previous subsection, the total current was concentrated within a very thin layer of the width $\tilde{\lambda}$. It was based on the assumption that the pinning force disappears when the vortex line leaves the small-size potential well, whereas inside the potential well the pinning force is very strong. As a result, outside the thin surface layers of the width $\tilde{\lambda}$ the vortex line consists of two straight segments [Figs. 3(b) and 4]. In the general case, the distribution of the pinning force may be smoother and the shape of a vortex line is more complicated. In addition, interactions between the vortices may modify the barrier for flux creep as well. However, the tendency must be the same: the current confined in a narrow surface layer drives the end of a vortex line away from the potential well to the regions where the pinning force is weaker and the vortex line is quite straight with the length proportional to thickness of the film if the latter is thin enough. Therefore, the barrier height for the vortex jump is smaller for smaller d .

We also note that we do not consider an anisotropic case and limit our discussion to isotropic samples. The effect of anisotropy on the barrier height was considered in detail in Ref. 19. In the presence of anisotropy the circular loop becomes elliptic and the vortex-line tension ε must be replaced by some combination of vortex-line tensions for different crystal directions. These quantitative modifications are not essential for our qualitative analysis.

Our scenario assumes that the current is concentrated near the film surfaces. In general, width of the current layer may vary from $\tilde{\lambda}$ to effective Campbell length λ_C . One may then expect a *nonmonotonous* thickness dependence when λ_C is comparable with d . As we see, the Campbell length is an important quantity in determining whether current density

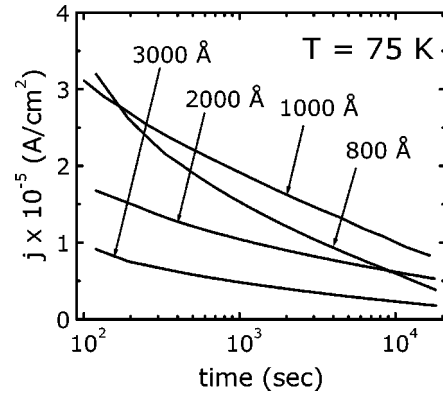


FIG. 6. Time evolution of the average persistent current density j_a at $T=75$ K for films of different thickness.

inhomogeneity must be taken into account or not (in the absence of the surface pinning). The length λ_C can be estimated from the microwave experiments: according to Golosovskii and co-workers²¹ $\lambda_C \approx 1000\sqrt{H}$ Å, where the field H is measured in tesla. For $H \approx 0.2$ T this results in $\lambda_C \approx 450$ Å or $2\lambda_C \approx 900$ Å, which has to be compared with the film thickness.

IV. COMPARISON WITH THE EXPERIMENT

A decrease of the measured current density with an increase of the film thickness is reported in numerous experimental works.^{6,10-12} This is consistent with the predictions given above for either surface or/and bulk pinning. Both pinning mechanisms predict similar $1/d$ dependence of j and it is, therefore, impossible to distinguish between surface and bulk pinning in this type of measurements. Only the additional information from the thickness dependence of the relaxation rate allows the drawing of some conclusions about the pinning mechanisms.

Magnetic relaxation measurements in films of different thickness are discussed in detail in Refs. 11 and 12. Using excerpts from the data reported there we demonstrate an agreement of these data with our theory.

Measurements were conducted on four 5×5 mm² YBa₂Cu₃O_{7- δ} films of thickness $2d=800, 1000, 2000,$ and 3000 Å, prepared by the laser ablation technique on SrTiO₃ substrates.¹⁴ All samples had $T_c \approx 89$ K. The morphology of the samples was examined by atomic-force microscopy (AFM) technique and was found to be similar: the average grain size $(1-50) \times 10^2$ Å and intergrain distance 50 Å (for a typical AFM picture of our samples, see Fig. 1(c) in Ref. 12). The magnetic moment was measured as a function of field, temperature and time, using a Quantum Design superconducting quantum interference device magnetometer.

The average persistent current density was extracted from the magnetic hysteresis loops using the Bean model adapted for our case: $j_a[A/cm^2] = 30M/da^3$, where $M[emu]$ is the irreversible magnetic moment, $d[cm]$ is a half of the film thickness and $a=0.5$ cm is the lateral dimension. Figure 5 shows the persistent current density j at $T=5$ K as a function of the applied magnetic field H . Apparently, j is larger in thinner films. The same trend is found at all temperatures. These observations are in good agreement with Eqs. (19) and

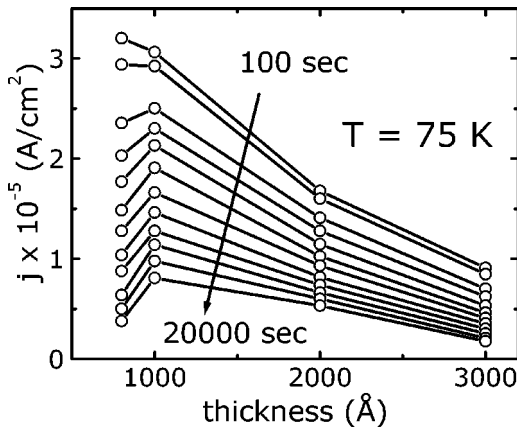


FIG. 7. Thickness dependence of the average persistent current density j_a at $T=75$ K taken at different times.

(26). We note, however, that since the value of j_s is not known, we cannot point out the dominance of pure surface, pure bulk or a mixed type of pinning. On the other hand, it is unlikely that the observed thickness dependence is due to changes in the density of pinning centers with thickness, since the films' morphology is similar for all of our samples. This is further indirectly confirmed by the relaxation measurements. The decrease of current density due to increase of a mean grain size in thicker films would simultaneously result in faster relaxation, contrary to our observations.

Figure 6 shows typical relaxation curves at $H=0.2$ T (ramped down from 1 T) measured in films of different thickness. The interesting and unexpected feature is that curves cross, i.e., the relaxation is faster in thinner films. This is further illustrated in Fig. 7 where j vs d is plotted at different times. At the beginning of the relaxation process, the average current density in the thinner films is larger. However, in the thinner films, the current density decreases much faster than in the thicker ones; as a result j_a exhibits a nonmonotonous dependence on thickness at later times, as shown in Fig. 7. The faster relaxation in thinner films is in qualitative agreement with our results, discussed in Sec. III, in particular in Secs. III B and III C. There, we find that such acceleration of the relaxation in thinner films may be understood only if we consider inhomogeneous bulk current density. In reality, it is very probable that *both* surface and bulk pinning mechanisms lead to inhomogeneous current density with a characteristic length scale in between the short (surface pinning) length $\tilde{\lambda}$ and the larger Campbell length.

V. SUMMARY AND CONCLUSIONS

Based on the two mode electrostatics approach we built a consistent theory of the critical state in thin type-II superconducting films *throughout the film thickness*. We show that, irrespective of the pinning mechanism, current density is always larger near the surface, and decays over a characteristic length scale, which is in between $\tilde{\lambda}$ (of order of the intervortex distance) and the Campbell length λ_C . The length scale $\tilde{\lambda}$ is determined by the (finite) vortex tension and by the boundary conditions which force vortices to be perpendicular to the surface of superconductor, whereas the Campbell length λ_C is determined by bulk pinning potential.

Following this physical picture we conclude that

(a) Current density and magnetic induction in thin films in perpendicular field are highly inhomogeneous throughout the film thickness. Surface pinning significantly enhances these inhomogeneities.

(b) Average current density decreases with the increase of film thickness approximately as $1/d$.

(c) Magnetic relaxation is *slower* in thinner films in the following cases: (1) In the absence of bulk pinning, i.e., only surface pinning is effective. (2) In the presence of bulk pinning, provided that the ratio between thickness and distance between neighboring defects is above a certain threshold ($d/a \sim 1$).

(d) Magnetic relaxation is *faster* in thinner films only if bulk pinning is effective and the ratio d/a is below this threshold.

In the experimental data presented here the measured average current j_a decreases with the increase of film thickness as predicted, and the relaxation rate is larger for the thinner films, suggesting that $d/a \sim 1$, and the effective distance between defects ≥ 1000 Å.

ACKNOWLEDGMENTS

We thank V. Vinokur, E. H. Brandt, L. Burlachkov, E. Zeldov, and M. Golosovskii for useful discussions. This work was supported in part by a grant from the Israel Science Foundation and the Heinrich Hertz Minerva Center for High Temperature Superconductivity, and in part by the German-Israeli Foundation under Grant No. 128-3-3/95. R.P. acknowledges support from the Clore Foundations. E.B.S. acknowledges a support by the Lady Davis Grant and thanks the Racah Institute of the Hebrew University for hospitality.

¹E. H. Brandt, Phys. Rev. B **54**, 4246 (1996); E. H. Brandt, Czech. J. Phys. **46**, 893 (1996).

²A. Gurevich and E. H. Brandt, Phys. Rev. Lett. **73**, 178 (1994); E. H. Brandt, *ibid.* **76**, 4030 (1996).

³E. H. Brandt and M. V. Indenbom, Phys. Rev. B **48**, 12 893 (1993); E. Zeldov, J. R. Clem, M. McElfresh, and M. Darwin, *ibid.* **49**, 9802 (1994); E. H. Brandt, Phys. Rev. Lett. **74**, 3025 (1995); J. McDonald and J. R. Clem, Phys. Rev. B **53**, 8643 (1996).

⁴C. Jooss, A. Forkl, and H. Kronmuller, Physica C **268**, 87 (1996).

⁵V. K. Vlasko-Vlasov, M. V. Indenbom, V. I. Nikitenko, A. A. Polyanskii, R. Prozorov, I. V. Grekhov, L. A. Delimova, I. A. Liniichuk, A. V. Antonov, and M. Y. Gusev, Supercond., Phys. Chem. Technol. **5**, 1582 (1992); V. K. Vlasko-Vlasov, L. A. Dorosinskii, M. V. Indenbom, V. I. Nikitenko, A. A. Polyanskii, and R. Prozorov, *ibid.* **6**, 555 (1993); R. Prozorov, A. A. Polyanskii, V. I. Nikitenko, I. V. Grehov, L. A. Delimova, and I. A. Liniychuk, *ibid.* **6**, 563 (1993); M. R. Koblishka, Physica C **259**, 135 (1996); M. R. Koblishka, A. J. J. van Dalen, and G. R. Kumar, J. Supercond. **9**, 143 (1996); M. R. Koblishka, Semi-

- cond. Sci. Technol. **9**, 271 (1996); T. Schuster, H. Kuhn, and E. H. Brandt, Phys. Rev. B **54**, 3514 (1996).
- ⁶C. Jooss, A. Forkl, R. Warthmann, H.-U. Habermeier, B. Leibold, and H. Kronmuller, Physica C **266**, 235 (1996).
- ⁷E. Zeldov, A. I. Larkin, V. B. Geshkenbein, M. Konczykowski, D. Majer, B. Khaykovich, V. M. Vinokur, and H. Shtrikman, Phys. Rev. Lett. **73**, 1428 (1994).
- ⁸W. T. Norris, J. Phys. D **3**, 489 (1970).
- ⁹M. McElfresh, T. G. Miller, D. M. Schaefer, R. Reifenberger, R. E. Muenchausen, M. Hawley, S. R. Foltyn, and X. D. Wu, J. Appl. Phys. **71**, 5099 (1992).
- ¹⁰L. Civale, T. K. Worthington, and A. Gupta, Phys. Rev. B **43**, 5425 (1991); D. Bhattacharia, P. Choudhury, S. N. Roy, and H. S. Maiti, J. Appl. Phys. **76**, 1120 (1994); A. Neminsky, J. Dumas, B. P. Thrane, C. Schlenker, H. Karl, and B. Stritzker, Phys. Rev. B **50**, 3307 (1994); A. Mongo-Campero, P. J. Bednarczyk, J. E. Tkaczyk, and J. A. DeLuca, Physica C **247**, 239 (1995).
- ¹¹R. Prozorov, E. Sheriff, Y. Yeshurun, and A. Shaulov, Physica C **282-287**, 2115 (1997).
- ¹²E. Sheriff, R. Prozorov, Y. Yeshurun, A. Shaulov, G. Koren, and C. Chabaud-Villard, J. Appl. Phys. **82**, 4417 (1997).
- ¹³E. H. Brandt, J. Low Temp. Phys. **64**, 375 (1986); P. H. Kes and R. Wordenweber, *ibid.* **67**, 1 (1987).
- ¹⁴G. Koren, E. Polturak, B. Fisher, D. Cohen, and G. Kimel, Appl. Phys. Lett. **53**, 2330 (1988).
- ¹⁵E. B. Sonin, A. K. Tagantsev, and K. B. Traito, Phys. Rev. B **46**, 5830 (1992); E. B. Sonin and K. B. Traito, *ibid.* **50**, 13 547 (1994).
- ¹⁶P. Mathieu and Y. Simon, Europhys. Lett. **5**, 67 (1988).
- ¹⁷E. H. Brandt, Phys. Rev. B **48**, 6699 (1993).
- ¹⁸B. Plaçais, P. Mathieu, Y. Simon, E. B. Sonin, and K. B. Traito, Phys. Rev. B **54**, 13 083 (1996).
- ¹⁹E. B. Sonin, Physica B **210**, 234 (1995).
- ²⁰E. B. Sonin and B. Horovitz, Phys. Rev. B **51**, 6526 (1995).
- ²¹M. Golosovskii, M. Tsindlekht, and D. Davidov, Semicond. Sci. Technol. **9**, 1 (1996).